

## SHORT REVIEW

# RELATION BETWEEN PHYSIOLOGICAL FUNCTION AND ENERGY METABOLISM IN THE CENTRAL NERVOUS SYSTEM

LOUIS SOKOLOFF

Laboratory of Cerebral Metabolism, U.S. Department of Health, Education, and Welfare,  
Public Health Service, Bethesda, MD 20014, U.S.A.

THE BRAIN is a complex organ composed of many structural and functional components with markedly different and independently regulated levels of functional and metabolic activity. In more homogeneous organs that do readily recognizable physical and chemical work, such as the heart, skeletal muscle, and kidney, a close relationship between functional activity and energy metabolism is well established. The existence of a similar relationship in the tissues of the CNS has been more difficult to prove, partly because of uncertainty about the nature of the work associated with nervous functional activity, but mainly because of the difficulty in assessing the levels of functional and metabolic activities in the same functional component of the brain at the same time. Pathological and pharmacological conditions with gross and diffuse effects on cerebral functional activity, particularly those that alter the level of consciousness, have been shown to be associated with changes in overall cerebral metabolic rate (KETY, 1950, 1957; LASSEN, 1959; SOKOLOFF, 1976), but such associations could reflect separate independent consequences of cellular dysfunction rather than a direct relationship between cerebral functional activity and energy metabolism. Changes in the metabolic rate of the brain as a whole have generally not been found during physiological alterations of cerebral functional activity (LASSEN, 1959; SOKOLOFF, 1969, 1976). What has clearly been needed is a method that measures the rates of energy metabolism in specific discrete regions of the brain in normal and altered states of functional activity. The recently developed [ $^{14}\text{C}$ ]deoxyglucose technique (SOKOLOFF *et al.*, 1977) appears to fulfill this need. It can be used to measure quantitatively the local rates of glucose utilization simultaneously in all the macroscopically visible structures of the brain. It can be applied to normal conscious animals as well as those under experimentally altered states of cerebral activity. Furthermore,

the [ $^{14}\text{C}$ ]deoxyglucose method employs an autoradiographic technique which provides pictorial representations of the relative rates of glucose utilization throughout the various components of the brain; even without quantification these autoradiographs provide clearly visible markers that map cerebral regions with increased or decreased rates of energy metabolism in altered physiological, pharmacological, and pathological states. This method has provided unequivocal evidence of a close relationship between functional activity and energy metabolism in discrete structural and/or functional units of the nervous system.

### METHODOLOGY

A full, detailed, and comprehensive description of the theoretical basis of the [ $^{14}\text{C}$ ]deoxyglucose method has recently been published (SOKOLOFF *et al.*, 1977). A brief summary of its essential principles is necessary, however, to clarify the salient features of its design, its rigid procedural requirements, and the limitations on its applications.

The method was designed to take advantage of the extraordinary spatial resolution afforded by a quantitative autoradiographic technique that was originally developed for the measurement of local cerebral blood flow (LANDAU *et al.*, 1955; REIVICH *et al.*, 1969). The dependence on autoradiography prescribed the use of radioactive substrates for energy metabolism, the labeled products of which could be assayed in the tissues by the autoradiographic technique. Although oxygen consumption is the most direct measure of energy metabolism, the volatility of oxygen and the short physical half-life of its radioactive isotopes precluded measurement of oxidative metabolism by the autoradiographic technique. In most circumstances glucose is almost the sole substrate for cerebral oxidative metabolism, and its utilization is stoichiometrically related to oxygen consumption (KETY, 1957; SOKOLOFF, 1976). Radioactive glucose is, however, not fully satisfactory because its labeled products have too short a biological half-life and are lost too rapidly from the cerebral tissues. The

*Abbreviations used:* DG, 2-deoxy-D-glucose; DG-6-P, 2-deoxy-D-glucose-6-phosphate.

labeled analogue of glucose, 2-deoxy-D-[ $^{14}\text{C}$ ]glucose, was, therefore, selected because it has some special biochemical properties that make it particularly appropriate to trace glucose metabolism and to measure the local rates of cerebral glucose utilization by the autoradiographic technique.

### Theory

The method is derived from a model based on the biochemical properties of 2-deoxyglucose (SOKOLOFF *et al.*, 1977). 2-Deoxyglucose is transported bi-directionally between blood and brain by the same carrier that transports glucose across the blood-brain barrier (BIDDER, 1968; BACHELARD, 1971; OLDENDORF, 1971). In the cerebral tissues it is phosphorylated by hexokinase (EC 2.7.1.1) to 2-deoxyglucose-6-phosphate (SOLS & CRANE, 1954). Deoxyglucose and glucose are, therefore, competitive substrates for both blood-brain transport and hexokinase-catalyzed phosphorylation.

during the interval of time equals the steady state flux of glucose through the hexokinase-catalyzed step times the duration of the interval, and the net rate of flux of glucose through this step equals the rate of glucose utilization.

These relationships can be mathematically defined and an operational equation derived if the following assumptions are made: (1) a steady state for glucose (i.e. constant plasma glucose concentration and constant rate of glucose consumption) throughout the period of the procedure; (2) homogeneous tissue compartment within which the concentrations of [ $^{14}\text{C}$ ]DG and glucose are uniform and exchange directly with the plasma; and (3) tracer concentrations of [ $^{14}\text{C}$ ]DG (i.e. molecular concentrations of free [ $^{14}\text{C}$ ]DG essentially equal to zero). The operational equation which defines  $R_i$ , the rate of glucose consumption per unit mass of tissues,  $i$ , in terms of measurable variables is as follows:

$$R_i = \frac{C_i^*(T) - k_1^* e^{-(k_2^* + k_3^*)T} \int_0^T C_p^* e^{(k_2^* + k_3^*)t} dt}{\left( \frac{\lambda V_m^* K_m}{\phi V_m K_m^*} \right) \left[ \int_0^T (C_p^*/C_p) dt - e^{-(k_2^* + k_3^*)T} \int_0^T (C_p^*/C_p) e^{(k_2^* + k_3^*)t} dt \right]} \quad (1)$$

Unlike glucose-6-phosphate, however, which is metabolized further eventually to  $\text{CO}_2$  and water and to a lesser degree via the hexosemonophosphate shunt, deoxyglucose-6-phosphate cannot be converted to fructose-6-phosphate and is not a substrate for glucose-6-phosphate dehydrogenase (SOLS & CRANE, 1954). There is very little glucose-6-phosphatase activity in brain (HERS, 1957) and even less deoxyglucose-6-phosphatase activity (SOKOLOFF *et al.*, 1977). Deoxyglucose-6-phosphate, once formed, is, therefore, essentially trapped in the cerebral tissues, at least long enough for the duration of the measurement. The half-lives of [ $^{14}\text{C}$ ]deoxyglucose-6-phosphate in the various cerebral tissues have been experimentally estimated; the average half-lives are 7.7 (S.D. =  $\pm 1.6$ ) and 9.7 (S.D. =  $\pm 2.6$ ) h in gray and white matter, respectively (SOKOLOFF *et al.*, 1977). The shortest half-life is 6.1 h in the inferior colliculus (SOKOLOFF *et al.*, 1977).

If the interval of time is kept short enough, for example, less than 1 h, to allow the assumption of negligible loss of [ $^{14}\text{C}$ ]DG-6-P from the tissues, then the quantity of [ $^{14}\text{C}$ ]DG-6-P accumulated in any cerebral tissue at any given time following the introduction of [ $^{14}\text{C}$ ]DG into the circulation is equal to the integral of the rate of [ $^{14}\text{C}$ ]DG phosphorylation by hexokinase in that tissue during that interval of time. This integral is in turn related to the amount of glucose that has been phosphorylated over the same interval, depending on the time courses of the relative concentrations of [ $^{14}\text{C}$ ]DG and glucose in the precursor pools and the Michaelis-Menten kinetic constants for hexokinase with respect to both [ $^{14}\text{C}$ ]DG and glucose. With cerebral glucose consumption in a steady state, the amount of glucose phosphorylated

where  $C_i^*(T)$  equals the combined concentrations of [ $^{14}\text{C}$ ]DG and [ $^{14}\text{C}$ ]DG-6-P in the tissue,  $i$ , at time,  $T$ , determined by quantitative autoradiography;  $C_p^*$  and  $C_p$  equal the arterial plasma concentrations of [ $^{14}\text{C}$ ]DG and glucose, respectively;  $k_1^*$ ,  $k_2^*$ , and  $k_3^*$  are the rate constants for the transport from the plasma to the tissue precursor pool, for the transport back from tissue to plasma, and for the phosphorylation of free [ $^{14}\text{C}$ ]DG in the tissue, respectively;  $\lambda$  equals the ratio of the distribution volume of [ $^{14}\text{C}$ ]DG in the tissue to that of glucose;  $\phi$  equals the fraction of glucose which once phosphorylated continues down the glycolytic pathway; and  $K_m^*$  and  $V_{\max}^*$  and  $K_m$  and  $V_{\max}$  are the familiar Michaelis-Menten kinetic constants of hexokinase for [ $^{14}\text{C}$ ]DG and glucose, respectively.

The rate constants are determined in a separate group of animals by a non-linear, iterative process which provides the least squares best-fit of an equation which defines the time course of total tissue  $^{14}\text{C}$  concentration in terms of the time, the history of the plasma concentration, and the rate constants to the experimentally determined time courses of tissue and plasma concentrations of  $^{14}\text{C}$  (SOKOLOFF *et al.*, 1977). The rate constants have thus far been determined only in normal conscious albino rats; the values obtained for  $k_1^*$ ,  $k_2^*$ , and  $k_3^*$  and their standard errors are  $0.189 \pm 0.012$ ,  $0.245 \pm 0.040$ , and  $0.052 \pm 0.010$  per min in gray matter and  $0.079 \pm 0.008$ ,  $0.133 \pm 0.046$ , and  $0.020 \pm 0.020$  per min in white matter, respectively (SOKOLOFF *et al.*, 1977). Preliminary estimates indicate that the values are quite similar in the conscious monkey (Kennedy, Sakurada, Shinohara, & Sokoloff, unpublished observations).

The  $\lambda$ ,  $\phi$ , and the enzyme kinetic constants are grouped together to constitute a single, lumped constant (see equation). It can be shown mathematically that this lumped constant is equal to the asymptotic value of the product of the ratio of the cerebral extraction ratios of [ $^{14}\text{C}$ ]DG and glucose and the ratio of the arterial blood to plasma specific activities when the arterial plasma [ $^{14}\text{C}$ ]DG concentrations is maintained constant. The lumped constant is also determined in a separate group of animals from arterial and cerebral venous blood samples drawn during a programmed intravenous infusion which produces and maintains a constant arterial plasma [ $^{14}\text{C}$ ]DG concentration (SOKOLOFF *et al.*, 1977). Thus far it has been determined only in the albino rat and the monkey. Values are 0.483 (s.e.m. =  $\pm 0.022$ ) in the rat (SOKOLOFF *et al.*, 1977) and 0.344 (s.e.m. =  $\pm 0.036$ ) in the monkey (Kennedy, Sakurada, Shinohara & Sokoloff, unpublished observations). The lumped constant appears to be characteristic of the species and does not appear to change significantly in a wide range of conditions (SOKOLOFF *et al.*, 1977).

Despite its complex appearance, equation (1) is really nothing more than a general statement of the standard relationship by which rates of enzyme-catalyzed reactions are determined from measurements made with radioactive tracers. The numerator of the equation represents the amount of radioactive product formed in a given interval of time; it is equal to  $C_T^*$ , the combined concentrations of [ $^{14}\text{C}$ ]DG and [ $^{14}\text{C}$ ]DG-6-P in the tissue at time,  $T$ , measured by the quantitative autoradiographic technique, less a term that represents the free unmetabolized [ $^{14}\text{C}$ ]DG still remaining in the tissue. The denominator represents the integrated specific activity of the precursor pool times a factor, the lumped constant, which is equivalent to a correction factor for an isotope effect. The term with the exponential factor in the denominator takes into account the lag in the equilibration of the tissue precursor pool with the plasma.

#### Procedure

Because local rates of cerebral glucose utilization are calculated by means of equation (1), this equation dictates the variables to be measured. The specific procedure employed is designed to evaluate these variables and to minimize potential errors that might occur in the actual application of the method. If the rate constants,  $k_1^*$ ,  $k_2^*$ , and  $k_3^*$ , are precisely known, then equation (1) is generally applicable with any mode of administration of [ $^{14}\text{C}$ ]DG and for a wide range of time intervals. At the present time the rate constants have been determined only in the conscious rat. These rate constants can be expected to vary with the condition of the animal, however, and for most accurate results should be re-determined for each condition studied. The structure of equation (1) suggests a more practicable alternative. All the terms in the equation that contain the rate constants approach zero with increasing time if the [ $^{14}\text{C}$ ]DG is so admin-

istered that the plasma [ $^{14}\text{C}$ ]DG concentration also approaches zero. From the values of the rate constants determined in normal animals and the usual time course of the clearance of [ $^{14}\text{C}$ ]DG from the arterial plasma following a single intravenous pulse at zero time, an interval of 30–45 min is adequate for these terms to become sufficiently small that considerable latitude in inaccuracies of the rate constants is permissible without appreciably increased error in the estimates of local glucose consumption (SOKOLOFF *et al.*, 1977). An additional advantage derived from the use of a single pulse of [ $^{14}\text{C}$ ]DG followed by a relatively long interval before killing the animal for measurement of local tissue  $^{14}\text{C}$  concentration is that by then most of the free [ $^{14}\text{C}$ ]DG in the tissues has been either converted to [ $^{14}\text{C}$ ]DG-6-P or transported back to the plasma; the optical densities in the autoradiographs then represent mainly the concentrations of [ $^{14}\text{C}$ ]DG-6-P and, therefore, reflect directly the relative rates of glucose utilization in the various cerebral tissues.

The experimental procedure is to inject a pulse of [ $^{14}\text{C}$ ]DG intravenously at zero time and to decapitate the animal at a measured time,  $T$ , 30–45 min later; in the interval timed arterial samples are taken for the measurement of plasma [ $^{14}\text{C}$ ]DG and glucose concentrations. Tissue  $^{14}\text{C}$  concentrations,  $C_T^*$ , are measured at time,  $T$ , by the quantitative autoradiographic technique. Local cerebral glucose utilization is calculated by equation (1) (SOKOLOFF *et al.*, 1977).

#### RATES OF LOCAL CEREBRAL GLUCOSE UTILIZATION IN THE NORMAL CONSCIOUS RAT

Thus far quantitative measurements of local cerebral glucose utilization have been completed only in the albino rat. These values are presented in Table 1. The rates of local cerebral glucose utilization in the normal conscious rat vary widely throughout the brain. The values in white structures tend to group together and are always considerably below those of gray structures. The average value in gray matter is approx 3 times that of white matter, but the individual values vary from approx 50 to 200  $\mu\text{mol}$  of glucose/100 g/min. The highest values are in the structures involved in auditory functions with the inferior colliculus clearly the most metabolically active structure in the brain.

Quantitative determinations of local cerebral glucose utilization in the normal conscious monkey are currently being carried out in this laboratory, and the values should be available soon. The results thus far indicate similar heterogeneity in the monkey brain, but the values are considerably lower, approximately one-third to one-half those in the rat, probably because of the lower cellular packing density and greater amounts of white matter (Kennedy, Sakurada, Shinohara & Sokoloff, unpublished observations).

## EFFECTS OF GENERAL ANESTHESIA

In the albino rat thiopental anesthesia reduces the rates of glucose utilization in all structures of the brain (Table 1). The effects are not uniform; the percent effects in white matter are relatively small compared to those in most gray structures. Anesthesia also markedly reduces the heterogeneity normally present within gray matter, an effect clearly visible in the autoradiographs (SOKOLOFF *et al.*, 1977). These results are in agreement with those of previous studies in which anesthesia has been found to decrease the cerebral metabolic rate of the brain as a whole (KETY, 1950; LASSEN, 1959; SOKOLOFF, 1976).

Preliminary studies indicate that thiopental anesthesia has effects in the rhesus monkey like those in the rat (SHAPIRO *et al.*, 1975). The effects of halothane anesthesia in the monkey are similar, except that it appears to leave the basal ganglia unaffected (SHAPIRO *et al.*, 1975). In contrast, phencyclidine, which is often used as an anesthetic agent but is probably a convulsant, causes 10–50% increases in glucose consumption in all gray structures, except the inferior colliculus, pontine nuclei, and cerebellar cortex where significant decreases are observed (SHAPIRO *et al.*, 1975).

## RELATION BETWEEN LOCAL FUNCTIONAL ACTIVITY AND ENERGY METABOLISM

The results of a variety of applications of the method demonstrate a clear relationship between local cerebral functional activity and glucose consumption. The most striking demonstrations of the close coupling between function and energy metabolism are seen with experimentally induced local alterations in functional activity that are restricted to a few specific areas in the brain. The effects on local glucose consumption are then so pronounced that they are not only observed in the quantitative results but can be visualized directly on the autoradiographs which are really pictorial representations of the relative rates of glucose utilization in the various structural components of the brain.

### *Effects of increased functional activity*

*Effects of sciatic nerve stimulation.* Electrical stimulation of one sciatic nerve in the rat under barbiturate anesthesia causes pronounced increases in glucose consumption (i.e. increased optical density in the autoradiographs) in the ipsilateral dorsal horn of the lumbar spinal cord (KENNEDY *et al.*, 1975).

*Effects of olfactory stimulation.* The [ $^{14}\text{C}$ ]deoxyglucose method has been used to map the olfactory system of the rat (SHARP *et al.*, 1975). Olfactory stimulation with amyl acetate has been found to produce increased labeling in localized regions of the olfactory bulb. Preliminary results obtained with other odors, such as camphor and cheese, suggest different spatial patterns of increased metabolic activity with different odors.

*Effects of experimental focal seizures.* The local injection of penicillin into the hand–face area of the motor cortex of the rhesus monkey has been shown to induce electrical discharges in the adjacent cortex and to result in recurrent focal seizures involving the face, arm, and hand on the contralateral side (CAVENESE, 1969). Such seizure activity causes selective increases in glucose consumption in areas of motor cortex adjacent to the penicillin locus and in small discrete regions of the putamen, globus pallidus, caudate nucleus, thalamus, and substantia nigra of the same side (Fig. 1) (KENNEDY *et al.*, 1975). Similar studies in the rat have led to comparable results and provided evidence on the basis of an evoked metabolic response of a ‘mirror’ focus in the motor cortex contralateral to the penicillin-induced epileptogenic focus (COLLINS *et al.*, 1976).

### *Effects of decreased functional activity*

Decrements in functional activity result in reduced rates of glucose utilization. These effects are particularly striking in the auditory and visual systems of the rat and the visual system of the monkey.

*Effects of auditory deprivation.* In the albino rat some of the highest rates of local cerebral glucose utilization are found in components of the auditory system, i.e. auditory cortex, medial geniculate ganglion, inferior colliculus, lateral lemniscus, superior olive, and cochlear nucleus (Table 1). The high metabolic activities of some of these structures are clearly visible in the autoradiographs (Fig. 2). Bilateral auditory deprivation by occlusion of both external auditory canals with wax markedly depresses the metabolic activity in all of these areas (Fig. 2) (Des Rosiers, Kennedy & Sokoloff, unpublished observations). The reductions are symmetrical bilaterally and range from 35 to 60%. Unilateral auditory deprivation also depresses the glucose consumption of these structures but to a lesser degree, and some of the structures are asymmetrically affected. For example, the metabolic activity of the ipsilateral cochlear nucleus equals 75% of the activity of the contralateral nucleus. The lateral lemniscus, superior olive, and medial geniculate ganglion are slightly lower on the contralateral side while the contralateral inferior colliculus is markedly lower in metabolic activity than the ipsilateral structure (Fig. 2). These results demonstrate that there is some degree of lateralization and crossing of auditory pathways in the rat.

*Visual deprivation in the rat.* In the rat, the visual system is 80–85% crossed at the optic chiasma (LASHLEY, 1934; MONTERO & GUILLERY, 1968), and unilateral enucleation removes most of the visual input to the central visual structures of the contralateral side. In the conscious rat studied 24 h after unilateral enucleation, there are marked decrements in glucose utilization in the contralateral superior colliculus, lateral geniculate ganglion, and visual cortex as compared to the ipsilateral side (Fig. 3) (KENNEDY *et al.*,

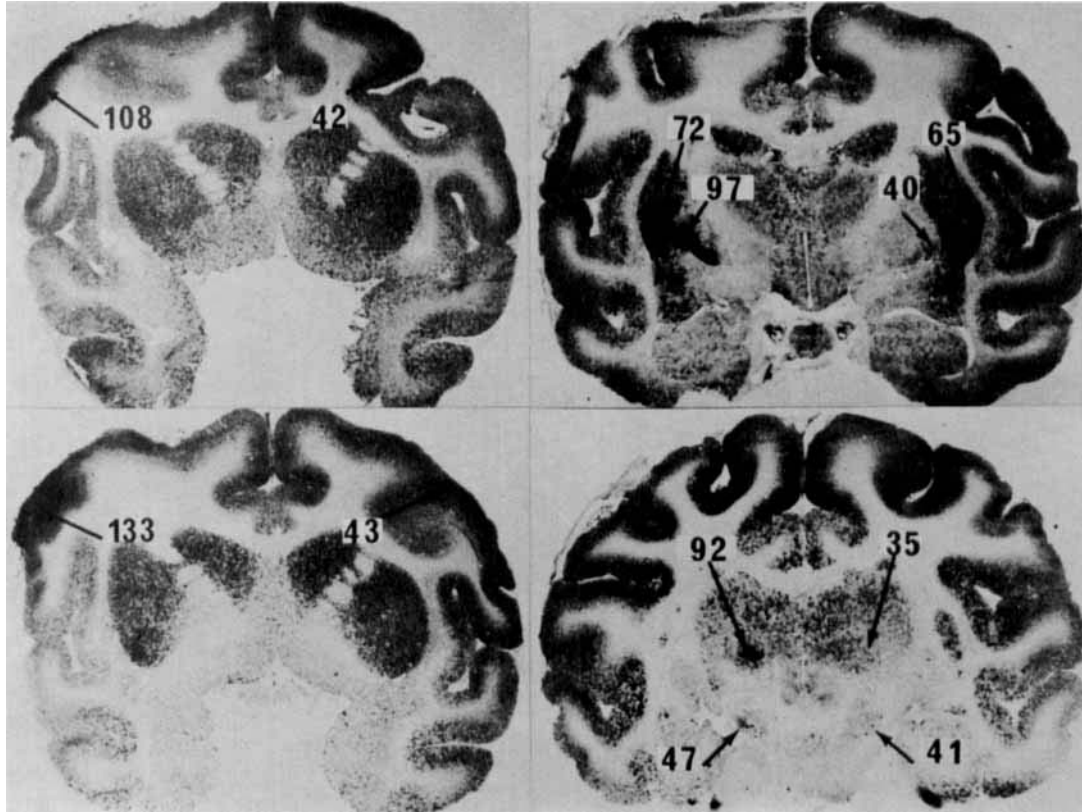
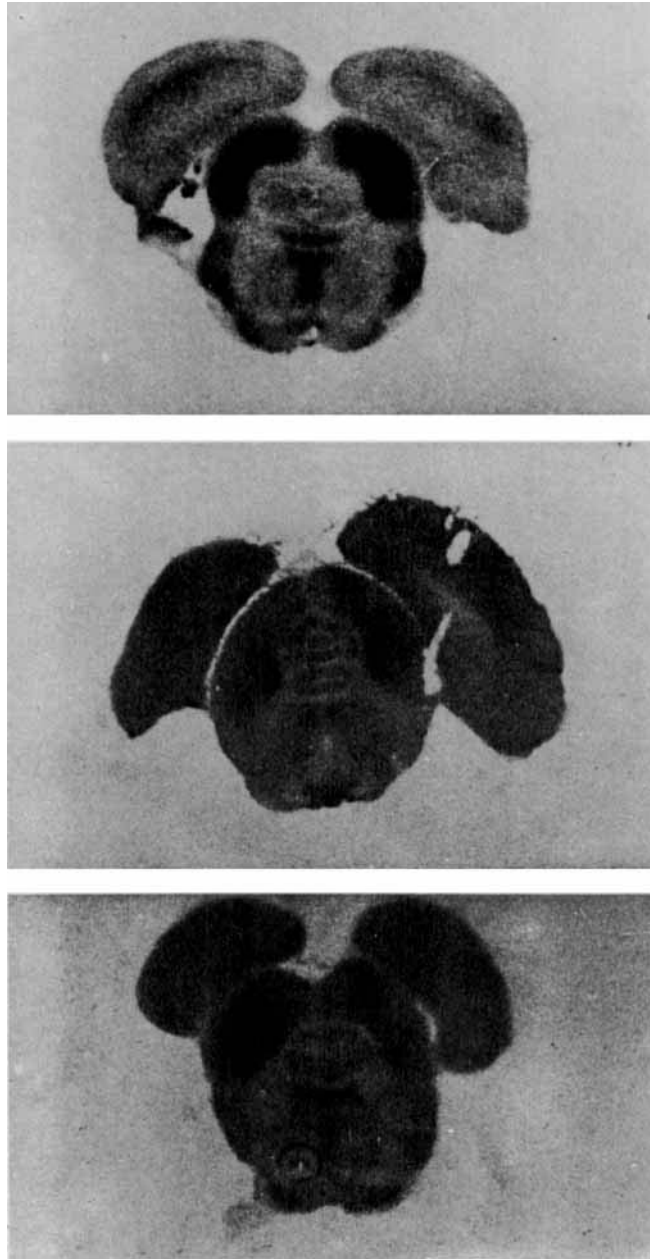


FIG. 1. Effects of focal seizures produced by local application of penicillin to motor cortex on local cerebral glucose utilization in the rhesus monkey. The penicillin was applied to the hand and face area of the left motor cortex. The left side of the brain is on the left in each of the autoradiographs in the figure. The numbers are the rates of local cerebral glucose utilization in  $\mu\text{mol}/100\text{ g tissue}/\text{min}$ . Note the following: *Upper left*, motor cortex in region of penicillin application and corresponding region of contralateral motor cortex; *Lower left*, ipsilateral and contralateral motor cortical regions remote from area of penicillin applications; *Upper right*, ipsilateral and contralateral putamen and globus pallidus; *Lower right*, ipsilateral and contralateral thalamic nuclei and substantia nigra. From KENNEDY *et al.* (1975).



**FIG. 2.** Effects of auditory deprivation on cerebral glucose utilization of some components of the auditory system of the albino rat. *Upper*, autoradiograph of section of brain from normal conscious rat with intact bilateral hearing in ambient noise of laboratory. The autoradiograph shows the inferior colliculi, the lateral lemnisci, and the superior olives, all of which exhibit bilateral symmetry of optical densities. *Middle*, autoradiograph of comparable section of brain from rat with bilateral occlusion of external auditory canals with wax and kept in sound-proof room. Note the virtual disappearance of the inferior colliculi, lateral lemnisci, and superior olives. *Lower*, autoradiograph of comparable section of brain from rat with one external auditory canal blocked. Note the asymmetry of the inferior colliculi, and the almost symmetrical intermediate reductions of densities in the lateral lemnisci and superior olives. The ear that was blocked was contralateral to the inferior colliculus that was markedly depressed. From Des Rosiers, Kennedy & Sokoloff (unpublished observations).

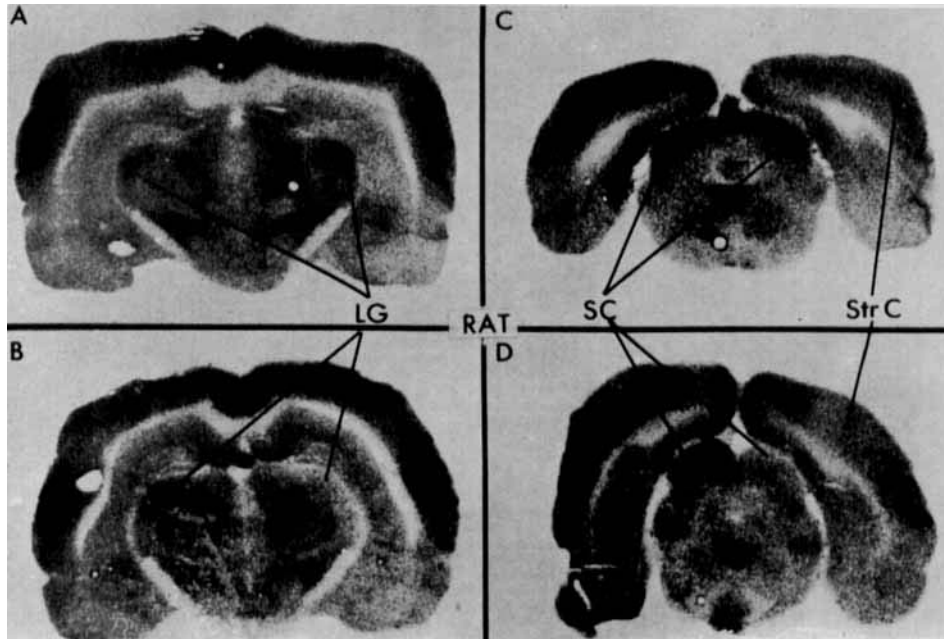


FIG. 3. Effects of unilateral enucleation on [ $^{14}\text{C}$ ]deoxyglucose uptake in components of the visual system in the rat. In the normal rat with both eyes intact the uptakes in the lateral geniculate bodies (LG), superior colliculi (SC) and striate cortex (STR C) are approximately equal on both sides (A and C). In the unilaterally enucleated rat there are marked decreases in optical densities in the areas corresponding to these structures on the side contralateral to the enucleation (B and D). From KENNEDY *et al.* (1975).

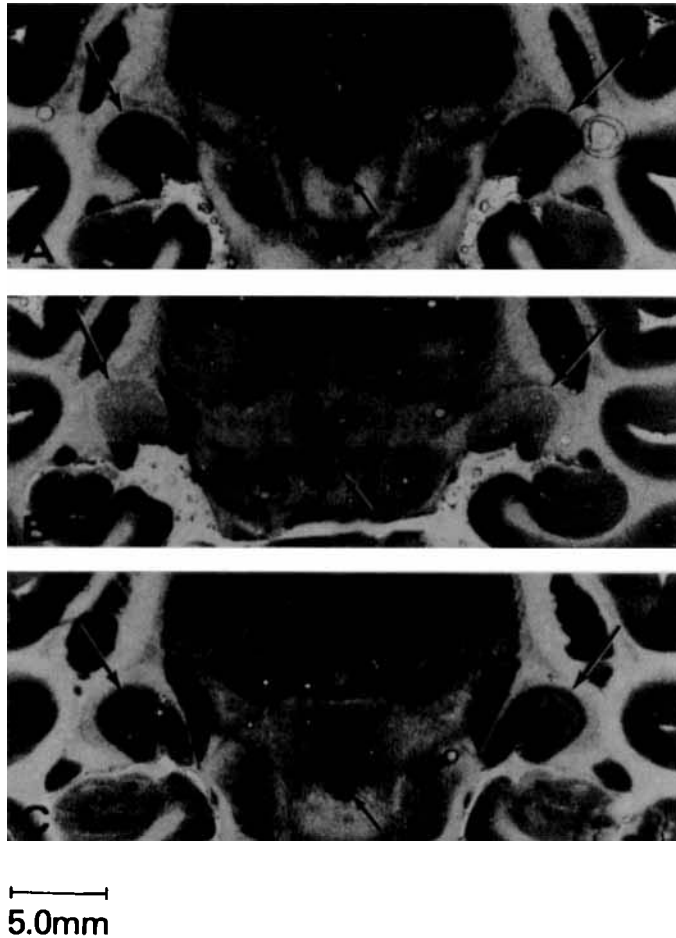


FIG. 4. Autoradiographs of coronal brain sections from rhesus monkeys at the level of the lateral geniculate bodies. Large arrows point to the lateral geniculate bodies; small arrows point to oculomotor nuclei. (A) Animal with intact binocular vision. Note the bilateral symmetry and relative homogeneity of the lateral geniculate bodies and oculomotor nuclei. (B) Animal with bilateral visual occlusion. Note the reduced relative densities, the relative homogeneity, and the bilateral symmetry of the lateral geniculate bodies and oculomotor nuclei. (C) Animal with right eye occluded. The left side of the brain is on the left side of the photograph. Note the laminae and the inverse order of the dark and light bands in the two lateral geniculate bodies. Note also the lesser density of the oculomotor nuclear complex on the side contralateral to the occluded eye. From KENNEDY *et al.* (1976).



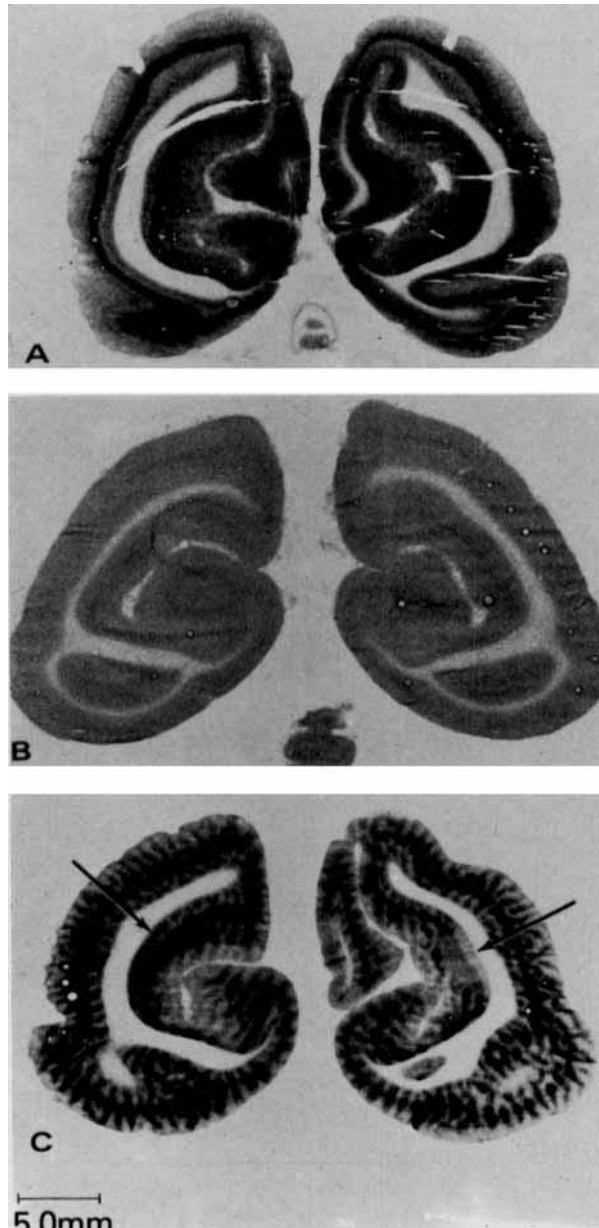


FIG. 5. Autoradiographs of coronal brain sections from rhesus monkeys at the level of the striate cortex. (A) Animal with normal binocular vision. Note the laminar distribution of the density; the dark band corresponds to Layer IV. (B) Animal with bilateral visual deprivation. Note the almost uniform and reduced relative density, especially the virtual disappearance of the dark band corresponding to Layer IV. (C) Animal with right eye occluded. The half-brain on the left side of the photograph represents the left hemisphere contralateral to the occluded eye. Note the alternate dark and light striations, each approx 0.3–0.4 mm in width, representing the ocular dominance columns. These columns are most apparent in the dark lamina corresponding to Layer IV but extend through the entire thickness of the cortex. The arrows point to regions of bilateral asymmetry where the ocular dominance columns are absent. These are presumably areas with normally only monocular input. The one on left, contralateral to occluded eye, has a continuous dark lamina corresponding to Layer IV which is completely absent on the side ipsilateral to the occluded eye. These regions are believed to be the loci of the cortical representations of the blind spots. From KENNEDY *et al.* (1976).

TABLE 1. NORMAL VALUES FOR LOCAL CEREBRAL GLUCOSE UTILIZATION IN THE CONSCIOUS AND THIOPENTAL-ANESTHETIZED ALBINO RAT\*§

| Structure                 | Local cerebral glucose utilization<br>( $\mu\text{mol}/100 \text{ g}/\text{min}$ ) |                   |          |
|---------------------------|--|-------------------|----------|
|                           | Control (6)†   | Anesthetized (8)† | % Effect |
|                           | Gray matter  |                   |          |
| Visual cortex             | 111 $\pm$ 5  | 64 $\pm$ 3        | -42      |
| Auditory cortex           | 157 $\pm$ 5  | 81 $\pm$ 3        | -48      |
| Parietal cortex           | 107 $\pm$ 3  | 65 $\pm$ 2        | -39      |
| Sensory-motor cortex      | 118 $\pm$ 3  | 67 $\pm$ 2        | -43      |
| Lateral geniculate body   | 92 $\pm$ 2   | 53 $\pm$ 3        | -42      |
| Medial geniculate body    | 126 $\pm$ 6  | 63 $\pm$ 3        | -50      |
| Thalamus: lateral nucleus | 108 $\pm$ 3  | 58 $\pm$ 2        | -46      |
| Thalamus: ventral nucleus | 98 $\pm$ 3   | 55 $\pm$ 1        | -44      |
| Hypothalamus              | 63 $\pm$ 3   | 43 $\pm$ 2        | -32      |
| Caudate-putamen           | 111 $\pm$ 4  | 72 $\pm$ 3        | -35      |
| Hippocampus: Ammon's horn | 79 $\pm$ 1   | 56 $\pm$ 1        | -29      |
| Amygdala                  | 56 $\pm$ 4   | 41 $\pm$ 2        | -27      |
| Cochlear nucleus          | 124 $\pm$ 7  | 79 $\pm$ 5        | -36      |
| Lateral lemniscus         | 114 $\pm$ 7  | 75 $\pm$ 4        | -34      |
| Inferior colliculus       | 198 $\pm$ 7  | 131 $\pm$ 8       | -34      |
| Superior olivary nucleus  | 141 $\pm$ 5  | 104 $\pm$ 7       | -26      |
| Superior colliculus       | 99 $\pm$ 3   | 59 $\pm$ 3        | -40      |
| Vestibular nucleus        | 133 $\pm$ 4  | 81 $\pm$ 4        | -39      |
| Pontine gray matter       | 69 $\pm$ 3   | 46 $\pm$ 3        | -33      |
| Cerebellar cortex         | 66 $\pm$ 2   | 44 $\pm$ 2        | -33      |
| Cerebellar nucleus        | 106 $\pm$ 4  | 75 $\pm$ 4        | -29      |
|                           | White matter   |                   |          |
| Corpus callosum           | 42 $\pm$ 2   | 30 $\pm$ 2        | -29      |
| Genu of corpus callosum   | 35 $\pm$ 5   | 30 $\pm$ 2        | -14      |
| Internal capsule          | 35 $\pm$ 2   | 29 $\pm$ 2        | -17      |
| Cerebellar white matter   | 38 $\pm$ 2   | 29 $\pm$ 2        | -24      |

\* Determined at 30 min following pulse of [ $^{14}\text{C}$ ]deoxyglucose.

† The values are the means  $\pm$  standard errors obtained in the number of animals indicated in parentheses. All the differences are statistically significant at the  $P < 0.05$  level.

§ From SOKOLOFF *et al.* (1977).

1975). In the rat with both eyes intact, no asymmetry in the autoradiographs is observed (Fig. 3).

*Visual deprivation in the monkey.* In animals with binocular visual systems, such as the rhesus monkey, there is only approx 50% crossing of the visual pathways, and the structures of the visual system on each side of the brain receive equal inputs from both retinae. Although each retina projects more or less equally to both hemispheres, their projections remain segregated and terminate in six well-defined laminae in the lateral geniculate ganglia, three each for the ipsilateral and contralateral eyes (HUBEL & WIESEL, 1968, 1972; WIESEL *et al.*, 1974; RAKIC, 1976). This segregation is preserved in the optic radiations which project the monocular representations of the two eyes for any segment of the visual field to adjacent regions of Layer IV of the striate cortex (HUBEL & WIESEL, 1968, 1972). The cells responding to the input of each monocular terminal zone are distributed transversely through the thickness of the striate cortex resulting in a mosaic of columns, 0.3-0.5 mm in width, alternately representing the monocular inputs of the two eyes. The nature and distribution of these ocular dominance columns have previously been characterized by electrophysiological techniques (HUBEL &

WIESEL, 1968), Nauta degeneration methods (HUBEL & WIESEL, 1972), and by autoradiographic visualization of axonal and transneuronal transport of [ $^3\text{H}$ ]proline- and [ $^3\text{H}$ ]fucose-labeled protein and/or glycoprotein (WIESEL *et al.*, 1974; RAKIC, 1976). Bilateral or unilateral visual deprivation, either by enucleation or by the insertion of opaque plastic discs, produce consistent changes in the pattern of distribution of the rates of glucose consumption, all clearly visible in the autoradiographs, that coincide closely with the changes in functional activity expected from known physiological and anatomic properties of the binocular visual system (KENNEDY *et al.*, 1976).

In animals with intact binocular vision no bilateral asymmetry is seen in the autoradiographs of the structures of the visual system (Figs. 4A, 5A). The lateral geniculate ganglia and oculomotor nuclei appear to be of fairly uniform density and essentially the same on both sides (Fig. 4A). The visual cortex is also the same on both sides (Fig. 5A), but throughout all of Area 17 there is heterogeneous density distributed in a characteristic laminar pattern. These observations indicate that in animals with binocular visual input the rates of glucose consumption in the visual pathways are essentially equal on both sides

of the brain and relatively uniform in the oculomotor nuclei and lateral geniculate ganglia, but markedly different in the various layers of the striate cortex.

Autoradiographs from animals with both eyes occluded exhibit generally decreased labeling of all components of the visual system, but the bilateral symmetry is fully retained (Figs. 4B, 5B), and the density within each lateral geniculate body is for the most part fairly uniform (Fig. 4B). In the striate cortex, however, the marked differences in the densities of the various layers seen in the animals with intact bilateral vision (Fig. 5A) are virtually absent so that, except for a faint delineation of a band within Layer IV, the concentration of the label is essentially homogeneous throughout the striate cortex (Fig. 5B).

Autoradiographs from monkeys with only monocular input because of unilateral visual occlusion exhibit markedly different patterns from those described above. Both lateral geniculate bodies exhibit exactly inverse patterns of alternating dark and light bands corresponding to the known laminae representing the regions receiving the different inputs from the retinae of the intact and occluded eyes (Fig. 4C). Bilateral asymmetry is also seen in the oculomotor nuclear complex; a lower density is apparent in the nuclear complex contralateral to the occluded eye (Fig. 4C). In the striate cortex the pattern of distribution of the [ $^{14}\text{C}$ ]DG-6-P appears to be a composite of the patterns seen in the animals with intact and bilaterally occluded visual input. The pattern found in the former regularly alternates with that of the latter in columns oriented perpendicularly to the cortical surface (Fig. 5C). The dimensions, arrangement, and distribution of these columns are identical to those of the ocular dominance columns described by Hubel and Wiesel (HUBEL & WIESEL, 1968, 1972; WIESEL *et al.*, 1974). These columns reflect the interdigitation of the representations of the two retinae in the visual cortex. Each element in the visual fields is represented by a pair of contiguous bands in the visual cortex, one for each of the two retinae or their portions that correspond to the given point in the visual fields. With symmetrical visual input bilaterally, the columns representing the two eyes are equally active and, therefore, not visualized in the autoradiographs (Fig. 5A). When one eye is blocked, however, only those columns representing the blocked eye become metabolically less active, and the autoradiographs then display the alternate bands of normal and depressed activities corresponding to the regions of visual cortical representation of the two eyes (Fig. 5C).

There can be seen in the autoradiographs from the animals with unilateral visual deprivation a pair of regions in the folded calcarine cortex that exhibit bilateral asymmetry (Fig. 5C). The ocular dominance columns are absent on both sides, but on the side contralateral to the occluded eye this region has the appearance of visual cortex from an animal with normal bilateral vision, and on the ipsilateral side this

region looks like cortex from an animal with both eyes occluded (Fig. 5). These regions are the loci of the cortical representation of the blind spots of the visual fields and normally have only monocular input (KENNEDY *et al.*, 1975, 1976). The area of the optic disc in the nasal half of each retina cannot transmit to this region of the contralateral striate cortex which, therefore, receives its sole input from an area in the temporal half of the ipsilateral retina. Occlusion of one eye deprives this region of the ipsilateral striate cortex of all input while the corresponding region of the contralateral striate cortex retains uninterrupted input from the intact eye. The metabolic reflection of this ipsilateral monocular input is seen in the autoradiograph in Fig. 5C.

The results of these studies with the [ $^{14}\text{C}$ ]deoxyglucose method in the binocular visual system of the monkey represent the most dramatic demonstration of the close relationship between physiological changes in functional activity and the rate of energy metabolism in specific components of the CNS.

#### PHARMACOLOGICAL STUDIES

The ability of the [ $^{14}\text{C}$ ]deoxyglucose method to map the entire brain for localized regions of altered functional activity on the basis of changes in energy metabolism offers a potent tool to identify the neural sites of action of agents with neuropharmacological and psychopharmacological actions. The method is still too new to have been extensively used for this purpose, but a number of such studies have been initiated, and preliminary reports have appeared.

The inhalation of 5-10%  $\text{CO}_2$ , which increases cerebral blood flow and produces desynchronization and a shift to higher frequency activity in the electroencephalogram, causes in the conscious rat moderate but diffuse reductions in local cerebral glucose utilization (DES ROSIERS *et al.*, 1976).

$\gamma$ -Hydroxybutyrate and  $\gamma$ -butyrolactone, which is hydrolyzed to  $\gamma$ -hydroxybutyrate in plasma, produce trance-like behavioral states associated with marked suppression of electroencephalographic activity (GIARMAN & ROTH, 1964). These effects are reversible, and these drugs have been used clinically as anesthetic adjuvants. There is evidence that these agents lower neuronal activity in the nigrostriatal pathway and may act by inhibition of dopaminergic synapses (ROTH, 1976). Studies in rats with the [ $^{14}\text{C}$ ]deoxyglucose technique have demonstrated that  $\gamma$ -butyrolactone produces profound dose-dependent reductions of glucose utilization throughout the brain (WOLFSON *et al.*, 1976). At the highest doses studied, 600 mg/kg of body weight, glucose utilization was reduced by approx 75% in gray matter and 33% in white matter, but there was no obvious further specificity with respect to the local cerebral structures affected. The reversibility of the effects and the magnitude and diffuseness of the depression of cerebral metabolic rate suggests that this drug might be considered as a chemical substitute for hypothermia in conditions in

which profound reversible reduction of cerebral metabolism is desired.

Ascending dopaminergic pathways appear to have a potent influence on glucose utilization in the forebrain of rats. Electrolytic lesions placed unilaterally in the lateral hypothalamus or pars compacta of the substantia nigra caused marked ipsilateral reductions of glucose metabolism in numerous forebrain structures rostral to the lesion, particularly the frontal cerebral cortex, caudate-putamen, and parts of the thalamus (SCHWARTZ *et al.*, 1976). Similar lesions in the locus coeruleus had no such effects.

Enhancement of dopaminergic synaptic activity by administration of the agonist of dopamine, apomorphine (WOLFSON & BROWN, 1976), or of amphetamine (Wechsler, Savaki & Sokoloff, unpublished observations), which stimulates release of dopamine at the synapse, produces marked increases in glucose consumption in some of the components of the extrapyramidal system known or suspected to contain dopamine-receptive cells. With both drugs, the greatest increases noted were in the zona reticulata of the substantia nigra and the subthalamic nucleus. Surprisingly, the caudate nucleus was unaffected, and reductions were noted in the suprachiasmatic nucleus of the hypothalamus and the habenula (Wechsler, Savaki & Sokoloff, unpublished observations).

The effects of the potent psychotomimetic agent D-lysergic acid diethylamide, have been examined in the rat (SHINOHARA *et al.*, 1976). In doses of 12.5–125 µg/kg, it caused dose-dependent reductions in glucose utilization in a number of cerebral structures. With increasing dosage more structures were affected and to a greater degree. There was no pattern in the distribution of the effects, at least none discernible at the present level of resolution, that might contribute to the understanding of the drug's psychotomimetic actions.

Acute morphine administration depresses glucose utilization in many areas of the brain, but the specific effects of morphine could not be distinguished from those of the hypercapnia produced by the associated respiratory depression (SAKURADA *et al.*, 1976). In contrast, morphine addiction, produced within 24 h by a single subcutaneous injection of 150 mg/kg of morphine base in an oil emulsion, reduces glucose utilization in a large number of gray structures in the absence of changes in arterial pCO<sub>2</sub>. White matter appears to be unaffected. Naloxone (1 mg/kg subcutaneously) reduces glucose utilization in a number of structures when administered to normal rats, but when given to the morphine-addicted animals produces an acute withdrawal-syndrome and reverses the reductions of glucose utilization in several of the structures, most strikingly in the habenula (SAKURADA *et al.*, 1976).

#### SUMMARY

The results of studies with the [<sup>14</sup>C]deoxyglucose technique unequivocally establish that functional ac-

tivity in specific components of the CNS is, as in other tissues, closely coupled to the local rate of energy metabolism. Stimulation of functional activity increases the local rate of glucose utilization; reduced functional activity depresses it. These changes are so profound that they can be visualized directly in autoradiographic representations of local tissue concentrations of [<sup>14</sup>C]deoxyglucose-6-phosphate. Indeed, the existence of such evoked metabolic responses to experimentally induced alterations in local functional activity, together with the ability to visualize them by the [<sup>14</sup>C]deoxyglucose method, has become the basis of a potent technique for the mapping of functional pathways in the CNS (KENNEDY *et al.*, 1975, 1976; PLUM *et al.*, 1976). The potential usefulness of this technique would be greatly advanced by technological improvements in the autoradiographic procedure that improve the spatial resolution to the microscopic or even the single-cell level.

*Acknowledgements*—The author wishes to express his appreciation to SUZANNE M. COOK for her valuable assistance in the preparation of this manuscript.

#### REFERENCES

- BACHELARD H. S. (1971) *J. Neurochem.* **18**, 213–222.  
 BIDDER T. G. (1968) *J. Neurochem.* **15**, 867–874.  
 CAVENESS W. F. (1969) in *Basic Mechanisms of the Epilepsies* (JASPER H. H., WARD A. A. & POPE A., eds.) pp. 517–534. Little, Brown, Boston.  
 COLLINS R. C., KENNEDY C., SOKOLOFF L. & PLUM F. (1976) *Arch Neurol.* **33**, 536–542.  
 DES ROSIERS M. H., KENNEDY C., SHINOHARA M. & SOKOLOFF L. (1976) *Neurology* **26**, 346.  
 GIARMAN N. J. & ROTH R. H. (1964) *Science* **145**, 583–584.  
 HERS H. G. (1957) *Le Métabolisme du Fructose*. p. 102. Editions Arscia, Bruxelles.  
 HUBEL D. H. & WIESEL T. N. (1968) *J. Physiol.* **195**, 215–243.  
 HUBEL D. H. & WIESEL T. N. (1972) *J. comp. Neurol.* **146**, 421–450.  
 KENNEDY C., DES ROSIERS M. H., REIVICH M., SHARP F., JEHL J. W. & SOKOLOFF L. (1975) *Science* **187**, 850–853.  
 KENNEDY C., DES ROSIERS M. H., SAKURADA O., SHINOHARA M., REIVICH M., JEHL J. W. & SOKOLOFF L. (1976) *Proc. natn. Acad. Sci., U.S.A.* **73**, 4230–4234.  
 KETY S. S. (1950) *Am. J. Med.* **8**, 205–217.  
 KETY S. S. (1957) in *The Metabolism of the Nervous System* (RICHTER D., ed.) pp. 221–237. Pergamon Press, London.  
 LANDAU W. H., FREYGANG W. H., ROWLAND L. P., SOKOLOFF L. & KETY S. S. (1955) *Trans. Am. Neurol. Ass.* **80**, 125–129.  
 LASHLEY K. S. (1934) *J. comp. Neurol.* **59**, 341–373.  
 LASSEN N. A. (1959) *Physiol. Rev.* **39**, 183–238.  
 MONTERO V. M. & GUILLERY R. W. (1968) *J. comp. Neurol.* **134**, 211–242.  
 OLDENDORF W. H. (1971) *Am. J. Physiol.* **221**, 1629–1638.  
 PLUM F., GJEDDE A. & SAMSON F. E. (1976) *Neurosci. Res. Prog. Bull.* **14**, 457–518.  
 RAKIC P. (1976) *Nature* **261**, 467–471.  
 REIVICH M., JEHL J. W., SOKOLOFF L. & KETY S. S. (1969) *J. Appl. Physiol.* **27**, 296–300.

- ROTH R. H. (1976) *Pharmac. Ther.* **2**, 71-88.
- SAKURADA O., SHINOHARA M., KLEE W. A., KENNEDY C. & SOKOLOFF L. (1976) *Neurosci. Abstr.* **2** (Part 1), 613.
- SCHWARTZ W. J., SHARP F. R., GUNN R. H. & EVARTS E. V. (1976) *Nature* **261**, 155-157.
- SHAPIRO H. M., GREENBERG J. H., REIVICH M., SHIPKO E., VAN HORN K. & SOKOLOFF L. (1975) in *Blood Flow and Metabolism in the Brain* (HARPER A. M., JENNETT W. B., MILLER J. D. & ROWAN J. O., eds.) pp. 9.42-9.43. Churchill Livingstone, Edinburgh.
- SHARP F. R., KAUFER J. S. & SHEPHERD G. M. (1975) *Brain Res.* **98**, 596-600.
- SHINOHARA M., SAKURADA O., JEHLI J. & SOKOLOFF L. (1976) *Neurosci. Abstr.* **2** (Part 1), 615.
- SOKOLOFF L. (1969) in *Psychochemical Research in Man* (MANDELL A. J. & MANDELL M. P., eds.) pp. 237-252. Academic Press, New York.
- SOKOLOFF L. (1976) in *Basic Neurochemistry* (SIEGEL G. J., ALBERS R. W., KATZMAN R. & AGRANOFF B. W., eds.) 2nd ed, pp. 388-413. Little, Brown, Boston.
- SOKOLOFF L., REIVICH M., KENNEDY C., DES ROSIERS M. H., PATLAK C. S., PETTIGREW K. D., SAKURADA O. & SHINOHARA M. (1977) *J. Neurochem.* **28**, 897-916.
- SOLS A. & CRANE R. K. (1954) *J. biol. Chem.* **210**, 581-595.
- WIESEL T. N., HUBEL D. H. & LAM D. M. K. (1974) *Brain Res.* **79**, 273-279.
- WOLFSON L. I. & BROWN L. (1976) *Neurosci. Abstr.* **2** (Part 1), 510.
- WOLFSON L. I., SAKURADA O. & SOKOLOFF L. (1976) *Trans. Am. Soc. Neurochem.* **7**, 165.